Cerebral Cortex November 2015;25:4155–4168
doi:10.1093/cercor/bhu134
Advance Access publication June 16, 2014

The Resting Brain of Alcoholics

Eva M. Müller-Oehring[1,2], Young-Chul Jung[2,3], Adolf Pfefferbaum[1,2], Edith V. Sullivan[2] and Tilman Schulte[1]

[1]Neurosci Program, Center for Health Sciences, SRI International, Menlo Park, CA, [2]Department of Psychiatry & Behavioral Sciences, Stanford University, Stanford, CA and [3]Department of Psychiatry, Yonsei University College of Medicine, Seoul, South Korea

Address correspondence to Dr Eva M. Müller-Oehring, Department of Psychiatry & Behavioral Sciences (MC 5723), Stanford University School of Medicine, 401 Quarry Road, Stanford, CA 94305-5723, USA. Email: evamoe@stanford.edu

Chronic alcohol consumption affects multiple cognitive processes supported by far-reaching cerebral networks. To identify neurofunctional mechanisms underlying selective deficits, 27 sober alcoholics and 26 age-matched controls underwent resting-state functional magnetic resonance imaging and neuropsychological testing. Functional connectivity analysis assessed the default mode network (DMN); integrative executive control (EC), salience (SA), and attention (AT) networks; primary somatosensory, auditory, and visual (VI) input networks; and subcortical reward (RW) and emotion (EM) networks. The groups showed an extensive overlap of intrinsic connectivity in all brain networks examined, suggesting overall integrity of large-scale functional networks. Despite these similar patterns, connectivity analyses identified network-specific differences of weaker within-network connectivity and expanded connectivity to regions outside the main networks in alcoholics compared with controls. For AT and VI networks, better task performance was related to expanded connectivity in alcoholism, supporting the concept of network expansion as a neural mechanism for functional compensation. For default mode, SA, RW, and EC networks, both weaker within-network and expanded outside-network connectivity correlated with poorer performance and mood. Current smoking contributed to some of these abnormalities in connectivity. The observed pattern of resting-state connectivity might reflect neural vulnerability of intrinsic networking in alcoholics and suggests a mechanism to explain signature impairments in EM, RW evaluation, and EC ability.

Keywords: alcoholism, cerebral networks, cognition and emotion, fMRI, resting-state functional connectivity

Introduction

Alcohol use disorder is a worldwide problem and the number 1 substance abuse problem in the United States of America (WHO 2011). It affects multiple cognitive processes of attention (AT), emotion (EM), and decision making supported by far-reaching neural networks (Bechara 2005; Loeber et al. 2009a, 2009b; Pfefferbaum et al. 2011). Various intrinsic connectivity networks have been identified in the resting brain (Andrews-Hanna et al. 2010; Laird et al. 2011) and have been linked to specific neuropsychiatric disorders (Anticevic et al. 2012, 2014). Their potential disruption from chronic alcoholism is only now emerging.

Brain functional networks disrupted in alcoholism (Kamarajan et al. 2004; Parks et al. 2010; Beck et al. 2012) include the default mode network (DMN) (Chanraud et al. 2011, 2012), the reward (RW) network (Park et al. 2010; Camchong et al. 2013b; Müller-Oehring et al. 2013), and the salience (SA) network (Sullivan et al. 2013). Camchong et al. (2013a, 2013c) focused on resting-state connectivity in RW and executive control (EC) networks in short- and long-term abstinent alcoholics and provided support for the assumed relationship between functional connectivity measures and relapse risk. Park et al. (2010) studied functional network connectivity in relation to RW prediction errors in alcoholics and found that abnormal connectivity between striatum and dorsolateral prefrontal cortex (dlPFC) predicted impairment in learning and the magnitude of alcohol craving. Similarly, Courtney et al. (2013) found that weaker frontostriatal connectivity during a response inhibition task was related to greater dependence severity in alcoholics. In our own studies, alcoholics, relative to controls, activated midbrain regions of the RW network more and showed weaker midbrain connectivity to medial and dorsolateral PFC during processing alcohol-related and negative emotional Stroop words (Müller-Oehring et al. 2013) and greater midbrain-striato-supplementary motor area (SMA) connectivity during a Stroop task (Schulte et al. 2012). Weaker striatal-prefrontal and greater midbrain-striatal-SMA connectivity within RW and motivation circuits in tasks with EC demands may be interpreted as altered networking underlying incentive SA for alcohol stimuli in alcoholism (Berridge and Robinson 1998; Yoder et al. 2009; Müller-Oehring et al. 2013).

Schulte at al. (2012) further observed the expected posterior cingulate cortex (PCC) deactivation in healthy subjects when focusing on tasks of high attentional load, whereas alcoholics failed to exhibit Stroop task-induced PCC deactivation. Thus, during task processing, alcoholics were less able to suppress activity in regions typically active during rest. The PCC is considered a hub involving both resting-state and task-related networks that function together to support complex behavior (Leech et al. 2011). The idea that differences in brain activity and in the functional synchrony between brain regions during the resting state in alcoholism may be compensatory and bestow resources for task processing was supported by the studies of Chanraud et al. (2011, 2012) and Marinkovic et al. (2009). Also Parks et al. (2010) and Rogers et al. (2012) observed compromised frontocerebellar functional connectivity in recently abstinent alcoholic patients and recruitment of additional brain areas for the performance of a simple motor task. Recruitment of additional areas and spatially expanded connectivity, however, may not always indicate functional compensation and the ability to engage brain reserve. For example, when a specific pattern of intrinsic functional connectivity signifies neural coherence necessary for network efficiency, extended activity to other regions can be a failure to keep neural coherence confined to that specific network and result in poor performance levels. Such forms of network dedifferentiation have been reported in normal aging (Reuter-Lorenz et al. 2000; Cabeza 2002; Cabeza et al. 2002, 2005), and in alcoholism where dedifferentiated patterns of frontostriatal connectivity to task demands predicted

© The Author 2014. Published by Oxford University Press. All rights reserved.
For Permissions, please e-mail: journals.permissions@oup.com

impairments in learning and the magnitude of alcohol craving (Parks et al. 2010).

These and our own studies provide evidence for disruption of functional networks in alcoholism. Yet, a systematic study on the integrity or disruption of multiple resting-state brain networks in alcoholism in relation to cognition and EM function has not been done. Based on earlier findings suggesting that spontaneous fluctuations in the resting-state blood oxygen level–dependent (BOLD) signal contribute significantly to variability in behavior (Fox and Raichle 2007), we tested whether interregional network connectivity was related to neuropsychological performance and mood states. By simultaneously examining multiple intrinsic brain networks, we were in position to examine the brain's intrinsic functional architecture (Smith et al. 2009; Biswal et al. 2010), to discern their similarities and differences in alcoholics from controls, and to test their potential relevance for cognition and EM.

We hypothesized that the patterns of connectivity in alcoholics and controls can reveal distinctive neurobiological mechanisms: 1) "network deficiency," that is, less or weaker connectivity in alcoholics relative to controls that is related to poorer behavioral outcome; 2) "compensatory neural ability" and neural mechanism to overcome processing deficiencies in the main network regions, that is, additional or stronger interregional connectivity in alcoholics relative to controls that is associated with normal task performance; and 3) "network dedifferentiation," that is, when additional or stronger regional connectivity in alcoholics relative to controls is related to poorer behavioral outcome.

Table 1
Study sample description: demographics, cognition, and emotion

Demographics, clinical characteristics	CTL	ALC	P
Women/men (*n*)	9/17	9/18	0.92[a]
Age (years)	49 ± 11	50 ± 9	0.76
Education (years)	16 ± 2	14 ± 2	*0.008*
Socioeconomic status	29 ± 13	40 ± 13	*0.003*
Handedness (Crovitz)	23 ± 11	24 ± 15	0.69
Visual acuity	1.9 ± 0.6	1.6 ± 0.5	0.31
Body mass index	27 ± 4	27 ± 7	0.76
Heart rate	72 ± 12	77 ± 11	0.11
Blood pressure			
Systolic	126 ± 14	128 ± 18	0.77
Diastolic	73 ± 7	76 ± 12	0.24
Age at alcoholism onset (years)	–	29 ± 13	–
Lifetime alcohol consumption (kg)	61 ± 93	926 ± 578	*0.0001*
AUDIT Score	2.5 ± 2	26.6 ± 9.5	*0.0001*
Alcohol Craving (ACQ-R) score	12.1 ± 7.6	7.8 ± 2.6	*0.002*
Cognition			
Verbal IQ (WTAR)	107 ± 12	100 ± 12	*0.036*
Digit Span, Total Score	17.6 ± 4.7	14.3 ± 3.5	0.007
Block Span, Total Score	17.5 ± 3.6	14.3 ± 2.3	0.001
Processing speed (MMSE)	0.17 ± 0.38	0.19 ± 0.4	0.87
Story memory (MMSE)	15 ± 6	12.8 ± 4.6	0.14
Trails A	24 ± 7	34 ± 15	*0.004*
Trails B	57 ± 25	84 ± 40	*0.007*
Emotion			
State Anxiety Score (STAI-S)	28 ± 8.6	33 ± 9.7	*0.032*
Trait Anxiety Score (STAI-T)	30 ± 7.2	42 ± 11.2	*0.0001*
Depressive Symptoms Score (BDI-II)	3 ± 3.2	11 ± 7.2	*0.0001*
Impulsivity Score (Barratt)	55 ± 8	63 ± 11	*0.004*
Self-esteem Score (Rosenberg)	26 ± 4.3	20 ± 5.4	*0.0001*

Note: Mean and standard deviation for each group: controls (CTL), and alcoholics (ALC); *t*-tests were applied to test for group differences; statistical significance level was set at $P < 0.05$ (italics).
SES, Socioeconomic Status: higher scores represent lower SES (range, 11–77) (Hollingshead and Redlich 1958), ACQ-R, Alcohol Craving Questionnaire (Drobes and Thomas 1999); IQ, Intelligence Quotient, *n*, number, Handedness Inventory: scores 14–32 right-handed, 50–70 left-handed (Crovitz and Zener 1962).
[a]χ^2 test.

Materials and Methods

Participants

Groups comprised 27 abstinent alcoholic men and 26 age-matched control men and women. Task-activated functional magnetic resonance imaging (fMRI) data from 26 alcoholics and 26 controls were published previously (Müller-Oehring et al. 2013). Alcoholics were recruited from local rehabilitation programs; controls were volunteers from the local community. All subjects were screened with the Structural Clinical Interview for DSM-IV (SCID) (First et al. 2012) and a clinical examination to rule out other Axis I diagnoses or nonalcohol substance abuse. In the alcoholic group, 26 participants met DSM-IV criteria for alcohol dependence and 1 participant met criteria for alcohol abuse. Of those meeting Dependence criteria, 26 were in early remission (met criteria within the past 12 months), while 1 was in sustained remission (>12 months, i.e., 375 days). The median number of weeks since alcoholics last met Dependence criteria was 17 weeks (mean = 16.0 weeks, standard deviation [SD] = 12.8 weeks). The median age of alcoholism onset was 25 years (mean = 29.1, SD = 13.6). Fifty percentage of alcoholics and 0% of controls met DSM-IV dependence for any type of drug dependence. The most common type of drug dependence among alcoholics was cocaine (endorsed by 35% of alcoholics), and the median number of weeks since last meeting drug dependence criteria was 102 weeks (mean = 452.5 weeks, SD = 532 weeks). In no case was drug dependence more recent than alcohol dependence. Significantly more alcoholics met DSM-IV criteria for current nicotine dependence (54%) than did controls (12%), $\chi^2(1) = 10.58$, $P = 0.003$ (Fisher's exact test). All participants gave written informed consent to participate in this study, which was approved by the Institutional Review Boards at SRI International and Stanford University School of Medicine.

Subject groups matched in age and handedness (23 right-handed subjects in each group; 2 nonright and 1 left-handed controls; and 1 nonright and 3 left-handed alcoholics) (Crovitz and Zener 1962) (Table 1). Groups also did not differ in VI acuity (Bach 2007), body mass index, and physiological measures including heart rate and blood pressure (Table 1). Additional clinical scales presented to all participants were the Alcohol Use Disorders Identification Test (AUDIT) (Babor et al. 2006), Short Item Scale Alcohol Craving Questionnaire-Revised Version (ACQ-R) (Drobes and Thomas 1999; Raabe et al. 2005); State-Trait Anxiety Inventory (STAI) (Spielberger 1983), Beck Depression Inventory (BDI-II) (Beck et al. 1996), Rosenberg Self-Esteem Scale (Rosenberg 1989), and the Barratt Impulsiveness Scale (Barratt et al. 1995). As expected, alcoholics exhibited higher AUDIT scores, greater state and trait anxiety, more depressive symptoms, higher impulsivity, and lower self-esteem than controls (Table 1).

Neuropsychological Assessment

The Wechsler Test of Adult Reading (WTAR) test (Wechsler 2001) was administered to estimate verbal intelligence quotients (IQ) and the Mini Mental State Exam subtests (MMSE-2 expanded version) (Folstein and Folstein 2010) to estimate processing speed and story memory. The Wechsler Memory Scale (Wechsler 1987) subtests provided estimates of verbal (digit span) and visuospatial (block span) working memory, and the Trail Making Test (Reitan and Wolfson 1985) for perceptual-motor processing speed (Trails A, B). Compared with age-matched controls, alcoholics had lower verbal IQ estimates, slower perceptual-motor processing speed (Trails A, B), and worse verbal (digit span) and visuospatial (block span) working memory. Alcoholics did not differ from controls in MMSE processing speed and story memory (Table 1).

Magnetic Resonance Imaging

Structural and functional magnetic resonance (MR) imaging data were acquired using a clinical whole-body GE 3T scanner. During the resting-state fMRI scan session, participants were instructed to lie

relaxed with their eyes open and not to think about anything in particular.

Data Acquisition and Analyses

Whole-brain structural and functional MRI data were acquired with an 8-channel head coil at a 3T GE whole-body scanner. Subject motion was minimized by following best practices for head fixation, and image series were inspected for residual motion. Whole-brain fMRI data were acquired with a T_2*-weighted gradient echo-planar pulse sequence (2D axial, echo time [TE] = 30 ms; repetition time [TR] = 2200 ms; flip angle = 90°; in-plane resolution = 3.75 mm; thick = 5 mm; skip = 0 mm; locations = 36; field of view [FOV] = 240 mm; number of excitations [NEX] = 1). A dual-echo fast spin-echo (FSE) sequence (2D axial; TR = 5000 ms; TE = 17/102 ms; thick = 5 mm; skip = 0 mm; *xy* matrix = 256; flip angle = 90°; locations = 36; FOV = 240 mm; 1 NEX) was used for spatially registering the fMRI data. A field map for correction of spatial distortions in the echo-planar images was generated from a gradient-recalled echo sequence pair (TR = 460 ms, TE = 3/5 ms, thickness = 5 mm, skip = 0 mm, locations = 36).

Image preprocessing was performed using the Statistical Parametric Mapping (SPM8) software package (Wellcome Department of Cognitive Neurology; www.fil.ion.ucl.ac.uk/spm/software/spm8/). The fMRI analysis focused on the whole brain. The functional images were subjected to geometric distortion (field map) correction and motion correction. The FSE structural images were co-registered to the mean unwarped and motion-corrected functional image for each subject, and functional and structural images were normalized to Montreal Neurological Institute (MNI) space. Normalized structural images were segmented into gray matter, white matter, and cerebrospinal fluid images. Functional volumes were smoothed with a Gaussian kernel of 8 mm full-width at half-maximum. Preprocessed individual images were then included into functional connectivity analysis for group comparison, using the SPM-based conn toolbox (www.nitrc.org/projects/conn/). Before averaging individual voxel data, the waveform of each brain voxel was filtered using a band-pass filter ($0.0083/s < f < 0.15/s$) to reduce the effect of low-frequency drift and high-frequency noise. Motion parameters were carefully considered in the analyses using the component-based noise correction method (CompCor) of noise reduction along with the efficient rejection of motion and artifactual time points allowing for better interpretation of functional connectivity results for correlated networks (Whitfield-Gabrieli and Nieto-Castanon, 2012). These images were then included in a second-level between-groups, random-effects analysis.

Seed Region Selection

Seed regions were selected from the automated anatomical labeling (aal) template (www.fil.ion.ucl.ac.uk/spm/ext/), which is an atlas widely used for manual macroanatomical parcellation of the single subject MNI-space template brain (Tzourio-Mazoyer et al. 2002) (www.gin.cnrs.fr/ spip.php?article217). For 7 networks, bilateral seed regions were selected from the aal template, and matched those reported by Raichle (2011): the PCC for the DMN, superior frontal gyri (SFG) for the EC network, anterior cingulate cortex (ACC) for the SA network, superior parietal lobe (SPL) for the dorsal AT network, postcentral gyrus (PCG) for the somatosensory (SS) network, Heschl's gyrus for the auditory (AU) network, and calcarine for the VI network. For the EM network, bilateral amygdala was selected from the aal template as seed region of interest (ROI) (Phan et al. 2002), and for the RW network the bilateral nucleus accumbens (NAcc) because it is considered a hub in the dopaminergic RW system (Demos et al. 2012). The NAcc seed region was built by using the MarsBaR toolbox in SPM to create 6 mm spherical ROI images centered at MNI coordinates $x = -9$, $y = 6$, $z = -4$ (left NAcc) and $x = 9$, $y = 6$, $z = -4$ (right NAcc) and based on anatomical coordinates defined in a stereotactic investigation of the human NAcc (Neto et al. 2008).

Second-Level Between-Groups, Random-Effects Analysis

Seed-to-voxel connectivity maps for each group were derived via individual time series correlations of activity over 135 time points, an index of synchronous activity. Within-group analyses were conducted where seed-to-voxel correlations for each group met a strict combined peak-and-extent threshold with a peak of $P \leq 0.001$ and, in addition, the cluster level (extent threshold) required a significance level of $P < 0.05$ Family-wise error (FWE) corrected for multiple comparison (reported in Table 2). Here, to test for group similarities in functional connectivity, conjunction analyses was performed identifying clusters of connectivity that can be observed in both groups, that is, the group overlap or similarity of the connectivity pattern. Further, to depict regions of "more or less expanded" connectivity, the within-group connectivity map of one group was masked by the connectivity map of the other group, thereby showing clusters of connectivity unique to that group. The focus of this study on the resting brain of alcoholics defined whether the respective masked analysis depicted clusters of "expanded" or "restricted" connectivity relative to controls. Also for the masked analyses, we used the strict statistical threshold that combined peak ($P_{peak} \leq 0.001$) and extent ($P_{FWE\text{-}corrected} < 0.05$), with the mask thresholded at $P = 0.05$ (reported in Table 3). Finally, to test for group differences in functional connectivity, between-group contrast analyses were performed with standard cluster-forming statistical thresholds for combined peak intensity and spatial extent set at peak threshold of $P_{uncorrected} < 0.01$ with an extent threshold of $P_{FWE\text{-}corrected} < 0.05$ (Poline et al. 1997) and reported in Table 4.

Statistical Analyses

To examine the relationships predicted between intrinsic network connectivity and clinical and behavioral measures, we used 2-tailed Pearson correlations in each group separately. Correlation analyses targeted the relationship between mood, performance, and connectivity strength for regions that differed by group either in extent or strength of connectivity. Significant Pearson correlations were confirmed by Spearman's Rho correlation coefficients. FDR correction for multiple correlations was performed for the number of cognitive and EM variables tested for each interregional connectivity measure, and reported in Tables 5 and 6 (Benjamini et al. 2001).

Results

Functional Brain Networks

Both groups showed largely overlapping seed-to-voxel connectivity maps for all networks tested (Table 2; Fig. 1). Group differences emerged for 6 of the 9 networks (Tables 3, and 4; Fig. 2): the default mode, EC, AT, SA, SS, and RW networks, but not for the EM, AU, and VI networks.

Self-Referential Network

Default Mode Network

Both groups showed PCC connectivity with lateral temporoparietal areas, medial and dorsolateral prefrontal cortices, and cerebellum. Relative to controls, alcoholics showed expanded PCC connectivity with right hippocampus, middle temporal gyrus and pole, and restricted PCC connectivity with right medial frontal gyrus (Table 3). The between-group contrast analysis (Table 4) revealed significantly greater PCC connectivity in alcoholics than controls to VI cortices and weaker connectivity to dorsal striatal regions including the caudate nucleus (head) and parts of the ACC (Fig. 2). Altered regional PCC connectivity in alcoholics was not correlated with performance and mood measures.

Cortical Integrative Function Networks

Executive Control Network

Both groups showed SFG connectivity with bilateral frontal, middle cingulate, lateral parietal and temporal cortices, and cerebellar regions. Alcoholics showed expanded SFG connectivity

Table 2
Functional network overlap in ALC and CTL

		K	BA/nucleus	*x*	*y*	*z*	*T*-score
Default mode network							
L	**PCC**/precuneus/hippocampal formation	**9691**	**23, 27**	**−6**	**−52**	**38**	**37.42**
L	Middle temporal/angular	3529	21, 39	−52	−60	18	11.63
L	Middle temporal/inferior temporal	993	20, 21	−56	−28	−8	5.33
R	Superior temporal /angular	2640	22, 39	56	−58	26	9.82
R	Middle temporal/inferior temporal	665	20, 21	68	−38	−2	4.56
L	Middle frontal/medial superior frontal	4048	46, 9, 10	−34	20	40	6.35
R	Middle frontal/superior frontal	931	46, 9	28	40	42	6.15
R	Cerebellum	222	Area 9	10	−52	−46	5.32[a]
Executive control network							
L	**SFG**/middle frontal /medial superior frontal	**25 110**	**8, 9, 10, 46**	**−22**	**48**	**36**	**20.35**
R	Angular/inferior parietal	1468	39, 40	50	−54	30	7.97
L	Angular/inferior parietal	1784	39, 40	−50	−64	38	6.71
L	PCC/middle cingulate cortex	1502	23	−6	−50	28	5.48
L	Cerebellum	275	Crus 2	−28	−82	−34	5.04
Salience network							
L	**ACC**/middle orbitofrontal/medial superior frontal/middle cingulate cortex/insula/caudate/putamen	**24 734**	**24, 32**, 10, 11, 23, 48	**−10**	**44**	**8**	**28.20**
R	Supramarginal/angular	239	39, 40, 42	54	−48	32	4.75
Attention network							
L	**SPL**/inferior parietal lobe	**17 949**	7, 40	**−24**	**−70**	**54**	**20.01**
R	Inferior temporal/fusiform	2242	20, 37	58	−56	−12	7.31
L	Precentral/middle frontal	1015	6, 8	−28	−4	48	7.26
R	Precentral/middle frontal	830	6	28	−4	42	7.13
R	Frontal inferior operculum	312	44	54	10	28	5.43
R	Frontal middle and inferior operculum	863	11, 47	30	38	−20	5.26
L	Precentral	350	6, 44	−48	4	24	5.06
R	Fusiform	378	37	30	−52	−16	4.98
Somatosensory network							
L	**Postcentral**/rolandic operculum/insula/superior, middle temporal/middle cingulate/supplementary motor area	**40 460**	**3, 4**, 6, 20, 21, 23, 43, 48	**−60**	**−6**	**16**	**20.91**
R	Lingual/inferior occipital and temporal	2283	18, 37	30	−96	−12	8.04
	Cerebellum	783	Area 8	12	−72	−48	5.92
Auditory network							
R	**Heschl**/rolandic operculum/superior temporal/paracentral/postcentral/thalamus	**33 550**	**48**, 41, 43, 3, 4	**46**	**−16**	**10**	**23.92**
R	ACC/medial prefrontal	242	10, 11, 24, 25	2	38	−2	5.51
Visual network							
R	**Calcarine**/inferior, middle, and superior occipital/fusiform/hippocampus/ parahippocampus/precuneus/angular	**26 638**	**17**, 18, 19, 20, 21, 30, 37, 7	**12**	**−80**	**8**	**23.05**
Reward network							
L	**NAcc**/caudate/putamen/insula/ACC/medial prefrontal	**11 317**	**25**, 10, 32, 48	**−8**	**6**	**−4**	**31.37**
Emotion network							
L	**Amygdala**/hippocampus, parahippocampus/inferior and middle temporal gyri and pole/midbrain	**21 404**	**34**, 20, 21, 38	**−26**	**0**	**−16**	**29.60**
R	Supplementary motor area	608	6	6	−14	58	4.78
R	Postcentral/rolandic operculum/superior temporal	770	43	58	−6	30	4.74

Note: Conjunction analysis: statistical significance (*T*-score) of clusters functionally connected to the cortical seed (bolded) in each group and their location in Montreal Neurological Institute (MNI) space (mm).

Functional connectivity network overlap using (exclusive) conjunction analysis with a combined peak-and-extend threshold set at peak $P < 0.001$ and extent $P_{FWE\text{-}corrected} < 0.05$.

[a]For regions with a significant peak threshold of $P_{FWE\text{-}corrected} < 0.05$; k = number of synchronously activated brain voxel.

with the cuneus, right superior temporal, and medial frontal gyri than controls, and restricted SFG connectivity with the left middle cingulate cortex (MCC), orbitofrontal regions, and the inferior parietal lobe (Table 3). The between-group contrast revealed significantly greater SFG connectivity strength with occipital areas including cuneus, fusiform, and VI association cortices in alcoholics (ALC) than controls (CTL), and weaker SFG connectivity strength with a right MCC region extending into the caudate body (Table 4).

Consistent with the dedifferentiation hypothesis, greater SFG-cuneus connectivity correlated with poorer visuospatial working memory (block span) (Table 5) and more depressive symptoms (BDI) (Table 6). Weaker SFG–MCC connectivity correlated with slower perceptual-motor processing speed (i.e., longer time to complete Trails A) (Table 5), higher anxiety, more depressive symptoms (Table 6), and younger age at alcoholism onset ($r = 0.43$, $P = 0.025$).

Salience Network

Both groups showed ACC connectivity with frontal and striatal brain regions; controls additionally exhibited ACC–bilateral temporoparietal cortical connectivity. Alcoholics showed expanded ACC connectivity with bilateral frontostriatal regions than controls and restricted connectivity with bilateral inferior parietal lobe (IPL), MCC, PCC, precuneus, and thalamus (Table 3). The between-group contrast revealed significantly greater ACC connectivity with frontalstriatal regions including the caudate head and inferior prefrontal, orbitofrontal, dorsal anterior cingulate cortices, and weaker ACC–thalamic connectivity in alcoholics than controls (Table 4).

Greater ACC–frontostriatal (IFG/caudate) connectivity in alcoholics correlated with poorer visuospatial working memory (block span), and more expanded ACC–frontostriatal (caudate/mFG) connectivity with slower perceptual-motor processing speed (Trails A). Weaker ACC–thalamus connectivity in alcoholics correlated with poorer verbal and visuospatial working memory (digit span and block span). In addition, more restricted ACC–thalamus, ACC–IPL, and ACC–MCC connectivity correlated with lower verbal and visuospatial working memory (Table 5).

Attention Network

Both groups showed SPL connectivity with precuneus, occipitotemporal, premotor, and prefrontal regions. Alcoholics

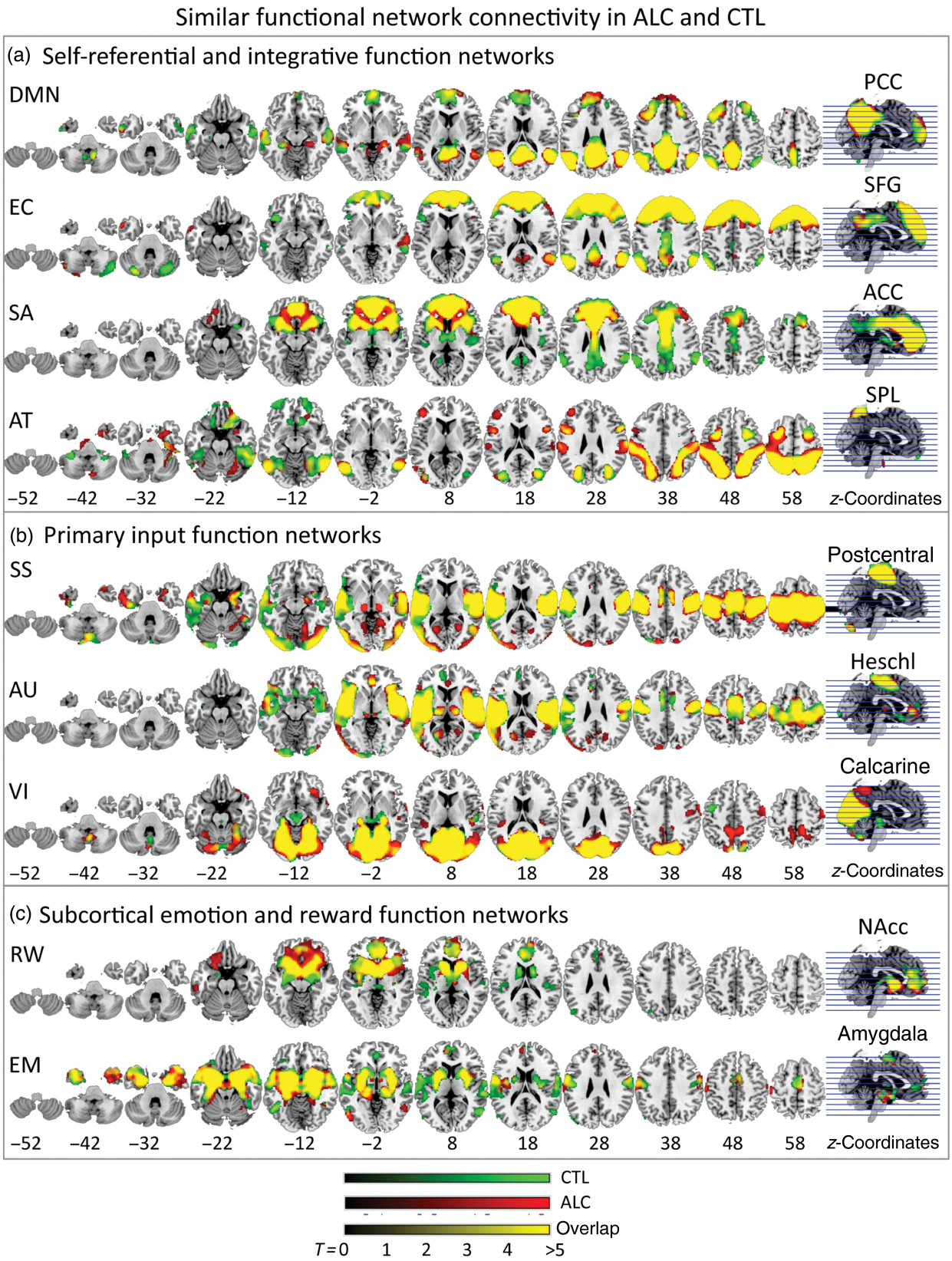

Figure 1. Intrinsic network similarities in alcoholics (ALC) and controls (CTL). (*a*) Self-referential default mode network (DMN) (posterior cingulate cortex seed, PCC) and integrative function networks: executive control (EC) network —superior frontal gyrus (SFG) seed, salience (SA) network—anterior cingulate cortex (ACC) seed, dorsal attention (AT) network —superior parietal lobe (SPL) seed; (*b*) primary input function networks: somatosensory (SS) network—postcentral gyrus seed, auditory (AU) network—Heschl gyrus seed, visual (VI) network—calcarine gyrus seed; and (*c*) subcortical emotion and reward networks: reward (RW) —nucleus accumbens (NAcc) seed, emotion (EM) —amygdala seed. A result output image was created for each within-group analysis for each seed's connectivity map with the same statistical threshold for all analyses (combined peak-and-extent threshold with peak $P < 0.001$ and extent $P_{FWE\text{-}corrected} < 0.05$). Brain regions showing synchronized BOLD activity with the seed are marked: red for ALC, green for CTL, and yellow when functionally connected in both groups (overlap). MNI *z*-coordinates indicate slice locations.

Table 3
Masked contrast analysis: statistical significance (*T*-score) of clusters (*k*) in ALC (relative to CTL) showing spatially "expanded" or "restricted" functional connectivity and their location in MNI space

Network-seed		*K*	BA/nucleus	*x*	*y*	*z*	*T*-score
Default mode network—PCC							
Expanded	R Hippocampus	182	20, 37	28	−30	−4	6.15[a]
	R Temporal (middle)	249	21	72	−24	−6	5.25
Restricted	L ACC, medial prefrontal	144	10, 32	4	48	16	6.27[a]
Executive control network—SFG							
Expanded	R Temporal (superior, middle), cuneus	151	21, 22	64	−18	−4	5.38[a]
	R Frontal (superior)	320	6, 8	20	4	52	4.95
Restricted	L Middle cingulate cortex (MCC)	624	23	−6	−16	38	7.17
	L Postcentral/IPL	185	2, 3	−48	−50	36	5.92[a]
	L Orbitofrontal	267	47	−42	20	−10	5.47
Salience network—ACC							
Expanded	L Orbitofrontal	1969	11, 47	−22	26	−6	7.93
Restricted	L IPL, angular	639	39, 40	−52	−54	42	6.77
	R IPL, supramarginal	175	40	56	−48	44	5.32
	R Frontal (medial superior)	409	9, 10	14	54	34	5.89
	R Middle cingulate cortex (MCC)	1357	23	14	−22	34	5.44
	L Thalamus	790		−6	−8	4	5.49
Attention network—SPL							
Expanded	L Precentral	1874	6	−28	−14	56	6.66
	R Postcentral	136	3, 4	34	−36	70	5.45[a]
	L Frontal (middle)	297	46	−38	44	28	5.02
	R Supramarginal/insula	360	40, 48	46	−30	32	4.72
	R Temporal pole	449	36	36	4	−36	4.72
Restricted	L Orbitofrontal/rectus	223	11	−2	54	−26	5.61[a]
	L Orbitofrontal	429	11	−18	22	−28	5.19
	L Cerebellum	191	Area 8	−34	−44	−44	5.40[a]
Somatosensory network—postcentral							
Expanded	L SPL	441	7	−30	−54	58	6.37
	L Occipital (superior)	356	19	−12	−92	36	6.21
	R Frontal (superior)	132	6	16	2	56	5.66[a]
	R SPL/IPL	330	7, 40	32	−52	56	5.58
	R Cerebellum/fusiform	1278	Area 6, 19	20	−62	−16	5.42
Restricted	L Temporoparietal junction	193	21, 39, 41	−46	−44	16	5.64[a]
	L Temporal (middle, inferior)	707	20	−58	−24	−18	4.97
Auditory network—Heschl							
Restricted	L Hippocampus	194	20	−34	−10	−16	6.19[a]
	L Olfactory	307	25	−2	16	−12	5.12
Visual network—calcarine							
Expanded	R Occipital (inferior)	648	19	48	−76	−10	6.02
	R Orbitofrontal	264	47	34	30	−14	5.98
	R Precuneus	742	5	14	−48	58	5.93
	R Postcentral	543	3	60	−12	48	5.29
Restricted	L Precentral	160	6	−42	0	46	5.68[a]
	L Midbrain	317	RN, STN	−2	−26	−4	5.44
Reward network—NAcc							
Expanded	R Olfactory/rectus/caudate	1434	11, 25	10	18	−14	7.24
	L Temporal (inferior, middle)	197	20	−56	−28	−18	5.54[a]
Restricted	L Amygdala	330	34	−22	−6	−12	9.74
	R Amygdala	261	34	22	−4	−14	6.70
	L Rolandic operculum	735	48	−46	−22	16	4.53
	L Angular	236	39	−46	−72	32	4.16
Emotion network—amygdala							
Expanded	L Postcentral	219	3	−52	−24	60	5.44[a]
Restricted	L MTG	287	21, 22	−50	−38	4	4.76

Note: Functional connectivity for masked contrast analysis using a combined peak-and-extend threshold of peak $P < 0.001$ and extent $P_{FWE\text{-}corrected} < 0.05$.
[a]For regions with a significant peak threshold of $P_{FWE\text{-}corrected} < 0.05$; k = number of synchronously activated brain voxel.

showed expanded SPL connectivity with left precentral and middle frontal gyri, bilateral postcentral and supramarginal gyri, and temporal cortex regions, and restricted SPL connectivity with left inferior frontal and orbitofrontal gyri, and to cerebellar regions (Table 3). The between-group contrast revealed significantly greater SPL–precentral gyrus connectivity in alcoholics than controls (Table 4); the large cluster included bilateral thalamus, left frontoparietal motor, premotor, SS, and superior temporal cortices, and the insula.

In contrast with the networks supporting the neural dedifferentiation hypothesis, for the AT network, more expanded SPL–left middle frontal gyrus (lMFG) connectivity in alcoholics correlated with fewer depressive symptoms (BDI) supporting the compensatory hypothesis (Table 6). More restricted SPL–cerebellar connectivity in alcoholics correlated with faster visuospatial coordination (Trails B) (Table 5).

"Overlay of self-referential and integrative function networks" revealed both segregated and partially overlapping networks, with regions selectively connected within one network and other regions linking 2 or more networks. The regions sharing connectivity with several networks were centered in the DMN: the PCC, cuneus, lateral parietal, and medial prefrontal regions (Fig. 2, left upper panel).

Primary Input Function Networks

Somatosensory Network

Both groups showed PCG connectivity with precentral regions with a large cluster extending frontally to SMAs, inferior and

Table 4

Group contrast analysis: Statistical significance (*T*-score) of clusters for differences between ALC and CTL in functional connectivity between the seed and the cluster location (*x y z*) in MNI space (mm)

		K	BA/nucleus	*x*	*y*	*z*	*T*-score
Default mode network—PCC							
ALC > CTL	R Occipital (inferior, middle, superior)	2794	18, 19	38	−86	4	3.91
CTL > ALC	R Caudate	1219		4	−2	20	5.31
Executive control network—SFG							
ALC > CTL	R Cuneus/occipital (middle, superior)	1187	18, 19	10	−80	22	4.08
CTL > ALC	R MCC/insula/caudate	3140	23, 48	16	−2	26	4.52
Salience network—ACC							
ALC > CTL	R Caudate/orbitofrontal/frontal (superior, medial)	1233	10, 11	16	26	0	4.55
	L Inferior orbitofrontal/caudate	1063	11, 47	−22	26	−6	4.45
CTL > ALC	R Thalamus	1271		12	−16	0	4.80
Attention network—SPL							
ALC > CTL	L Pre- and postcentral	3063	4, 6	−32	−18	68	4.50
Somatosensory network—postcentral							
ALC > CTL	R Cerebellum/lingual/calcarine	864[b]	area 4_5, 17	10	−48	−6	3.60
Reward network—NAcc							
CTL > ALC	L Amygdala, parahippocampus, hippocampus	512	20, 34, 35, 36	−22	−6	−12	6.13[a]
	L Angular/IPL	1385	7, 39	−48	−70	36	4.11

Note: For analysis group differences beween controls (CTL) and alcoholics (ALC), using a combined peak-and-extend threshold corrected for multiple comparisons $P_{FWE\text{-}corrected} < 0.05$ (Poline et al. 1997).
BA, Brodman area; PCC, posterior cingulate cortex; SFG, superior frontal gyrus; ACC, anterior cingulate cortex; SPL, superior parietal lobe; NAcc, nucleus accumbens, IPL, inferior parietal lobe.
[a]For regions with a significant peak threshold of $P_{FWE\text{-}corrected} < 0.05$.
[b]Region with trend at $P_{FWE\text{-}corrected} = 0.058$; *k*, number of synchronously activated brain voxel.

dorsolateral prefrontal regions, and posterior to supramarginal, temporal, and fusiform gyri, VI association areas, insula, and cerebellar regions. Alcoholics showed more expanded PCG connectivity with bilateral parietal lobes, left cuneus, superior and middle occipital gyrus, right lingual gyrus, and the cerebellum, and less expanded connectivity with the left temporoparietal junction (TPJ) and the left inferior temporal gyrus (Table 3). The between-group contrast revealed significantly greater PCG connectivity to bilateral occipital and cerebellar regions in alcoholics than controls (Table 4). More restricted postcentral–left TPJ connectivity in alcoholics correlated with lower self-esteem (Table 6).

None of the connectivity maps for seeds placed in Heschl's gyrus (AU network), or calcarine (VI network) revealed significant group differences. Here, groups exhibited similar resting-state connectivity maps with only some variation in their spatial extent.

Auditory Network

Both groups showed Heschl's gyrus connectivity with medial temporal cortex including insula, hypocampus, amygdala, and superior and middle temporal regions, to bilateral premotor and motor areas, to medial frontal areas including ACC, medial prefrontal and olfactory gyri, and to occipital regions including primary and secondary VI cortex, and the PCC. Although masked contrast analyses showed restricted connectivity to the left hippocampus and olfactory gyrus in alcoholics (Table 3), the between-group contrast did not reveal statistically different connectivity maps. No significant relationships to mood and performance measures were observed.

Visual Network

Both groups showed calcarine connectivity with bilateral occipital, medial temporal, medial inferior prefrontal, and left premotor cortices. Despite expanded calcarine connectivity with occipital, parietal, and right orbitofrontal regions, and restricted connectivity with left motor cortex and bilateral midbrain regions in alcoholics than controls (Table 3), the between-group contrast did not reveal statistically different calcarine functional connectivity strengths between groups. More expanded calcarine–inferior orbitofrontal connectivity in alcoholics correlated with better visuospatial working memory (block span) suggesting a positive effect from calcarine-based connectivity expansion on performance (Table 5), yet with less self-esteem (Table 6).

"Overlay of primary input function networks" revealed a segregated VI network and largely overlapping SS and AU networks. The main regions sharing connectivity within these primary input function networks were pre- and postcentral gyri and the insula (Fig. 2, left middle panel).

Subcortical Reward and Emotion Function Networks

Reward Network

Both groups showed NAcc connectivity with bilateral medial prefrontal regions including inferior prefrontal, orbitofrontal, and anterior cingulate regions, and with medial temporal regions including the insula, parahippocampal and entorhinal gyri, and the hippocampus. Masked contrast analyses revealed expanded NAcc connectivity with bilateral medial and inferior prefrontal gyri and left inferior temporal gyrus in alcoholics, and restricted connectivity with bilateral amygdala, left medial temporal, angular, and middle occipital gyri (Table 3). The between-group contrast revealed significantly weaker NAcc–amygdala and NAcc–angular gyrus connectivity in alcoholics than controls (Table 4).

More expanded NAcc–medial PFG connectivity in alcoholics correlated with higher trait anxiety scores and more restricted NAcc–left amygdala connectivity with higher alcohol craving (ACQ-R), significantly different from controls. Weaker NAcc–left amygdala connectivity correlated with lower self-esteem, and weaker NAcc–left IPL connectivity with more depressive symptoms (BDI), significantly different from controls (Table 6).

Emotion Network

Both groups showed amygdala connectivity with temporal, medial frontal, temporoparietal, extrastriate, and subcortical regions including the midbrain, thalamus in controls, pallidum and putamen in alcoholics. Despite more expanded amygdala–

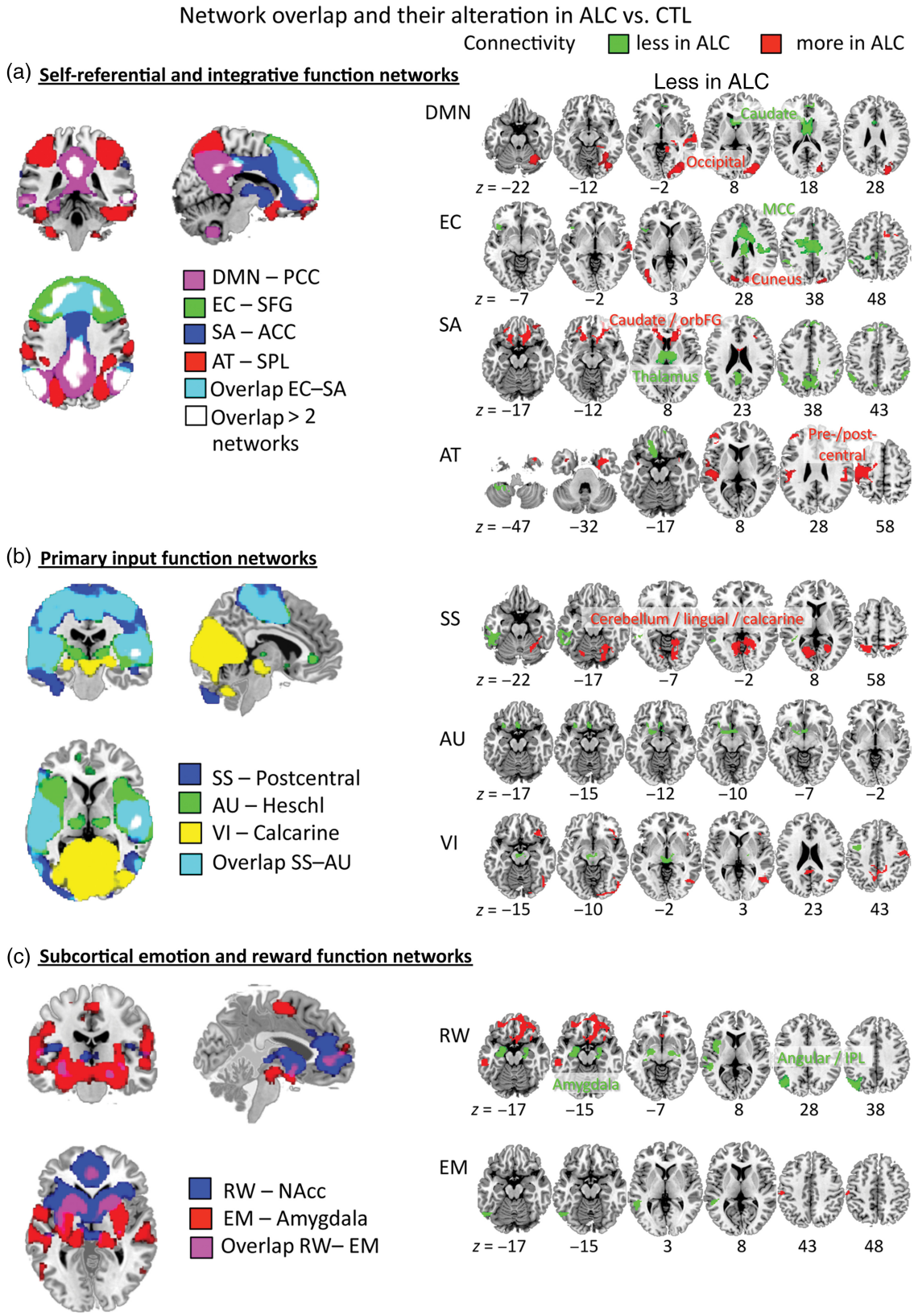

Figure 2. Intrinsic network differences in alcoholics (ALC) relative to controls (CTL). Left panels: Illustration of network segregation and overlap for (*a*) self-referential (DMN–PCC seed) and integrative function networks (EC–SFG seed, SA–ACC seed, AT–SPL seed), (*b*) primary input function networks (SS–postcentral seed, AU–Heschl seed, VI–calcarine seed), and (*c*) subcortical emotion and reward networks (RW–NAcc seed, EM–amygdala seed). A result output image was created from group conjunction analysis for each seed's connectivity map with the same statistical threshold for all analyses (combined peak-and-extent threshold with peak $P < 0.001$ and extent $P_{FWE\text{-}corrected} < 0.05$). Right panels: For each network, illustration of altered seed-to-voxel connectivity in ALC relative to CTL: marked red when "expanded" and green when "restricted" for masked contrast analysis (Table 3); for group contrast analysis (Table 4), regions are labeled in the figure and marked in red when ALC > CTL and green when CTL > ALC; combined peak-and-extent threshold corrected for multiple comparisons $P_{FWE\text{-}corrected} < 0.05$ (Poline et al. 1997). MNI *z*-coordinates indicate slice locations.

Table 5

Pearson correlation results between cognitive measures and connectivity strength in whole group (ALL), alcoholics (ALC), controls (CTL), and interactions between the 2 groups, for regions of interest (ROI) by group differences in functional connectivity

Analysis	Connectivity	Seed—ROI	Cognition		ALL	ALC	CTL	Interaction
Default mode network								
Group contrast	ALC > CTL	PCC—rMOG	Trails A	*R*	**0.40***	**0.45**	−0.07	***z* = 1.88**
				P	**0.003**	**0.019**	ns	**0.03**
Executive control network								
Group contrast	ALC > CTL	SFG—Cuneus	Block Span	*r*	**−0.42***	**−0.45**	0.03	***z* = −1.75**
				P	**0.002**	**0.019**	ns	**0.04**
	CTL > ALC	SFG—MCC	Trails A	*r*	**−0.46***	**−0.53***	0.05	***z* = −2.19**
				P	**0.001**	**0.005**	ns	**0.014**
Salience network								
Group contrast	ALC > CTL	ACC—IFC/caudate	Block Span	*r*	**−0.42***	**−0.39**	−0.03	*z* = −1.30
				P	**0.002**	**0.045**	ns	0.096
	CTL > ALC	ACC—Thalamus	Digit Span	*r*	**0.37***	**0.51***	−0.04	***z* = 2.05**
				P	**0.008**	**0.006**	ns	**0.02**
			Block Span	*r*	**0.36***	**0.46**	−0.05	***z* = 1.88**
				P	**0.01**	**0.016**	ns	**0.03**
Masked contrast	Expanded	ACC—Caudate/mFG	Trails A	*r*	**0.37***	**0.43**	−0.02	***z* = 1.64**
				P	**0.006**	**0.027**	ns	**0.05**
	Restricted	ACC—Thalamus	Digit Span	*r*	**0.37***	**0.50***	0.03	***z* = 1.78**
				P	**0.007**	**0.008**	ns	**0.038**
			Block Span	*r*	**0.32**	**0.46**	−0.09	***z* = 2.02**
				P	**0.02**	**0.015**	ns	**0.022**
		ACC—IPL	Block Span	*r*	**0.34**	**0.39**	−0.04	*z* = 1.54
				P	**0.016**	**0.048**	ns	0.062
		ACC—MCC/cuneus	Digit Span	*r*	0.26	**0.40**	−0.06	***z* = 1.64**
				P	0.062	**0.039**	ns	**0.05**
Attention network								
Masked contrast	Expanded	SPL—cerebellum-8	Trails B	*r*	0.11	**0.39**	0.13	*z* = 0.96
				P	ns	**0.045**	ns	0.17
Visual network								
Masked contrast	Expanded	Calcarine—Inf OFG	Block Span	*r*	−0.16	**0.51***	−0.20	***z* = 2.60**
				P	ns	**0.007**	ns	**0.0047**

Note: For ROIs derived from group contrast analysis (see Table 4) the direction of connectivity differences is indicated by *ALC > CTL* and *CTL > ALC*; for ROIs derived from masked contrast analysis (see Table 3) the direction of connectivity differences is indicated by *"expanded"* and *"restricted"* in ALC relative to controls.

PCC, posterior cingulate cortex; MCC, middle cingulate cortex; ACC, anterior cingulate cortex; SFG, superior frontal gyrus; mSFG, medial superior frontal gyrus; IFG, inferior frontal gyrus; mFG, medial frontal gyrus; Inf OFG, inferior orbitofrontal gyrus; IPL, inferior parietal lobe.

*Significant FDR corrected for multiple comparisons (Benjamini et al. 2001).

postcentral cortical and less expanded amygdala–left middle temporal gyrus (lMTG) connectivity in alcoholics (Table 3), no significant group differences emerged for amygdala-seeded connectivity maps. Also, significant relationships were not forthcoming between altered regional amygdala connectivity in alcoholics, performance, and mood measures.

"Overlay of subcortical RW and emotion function networks" revealed mainly segregated networks that shared functional connectivity in 2 regions: the caudate and medial prefrontal cortex (Fig. 2, left lower panel).

Premorbid Factors, Smoking, and Nonalcohol Drug Use

To test whether "potential premorbid differences" contributed to the observed group differences in functional network connectivity, we correlated verbal IQ, education, and socioeconomic status (SES) (Hollingshead and Redlich 1958) with interregional connectivity for regions showing group differences in strength and spatial extent (see Tables 3 and 4). Significant relationships were observed for verbal IQ (WTAR), an estimate of premorbid general cognitive ability.

For the DMN, lower verbal IQ in ALC was associated with weaker PCC–caudate (ALC: $r = 0.40$, $P = 0.038$; CTL: $r = -0.14$, ns; interaction: $z = 2.74$, $P = 0.006$) and more expanded PCC–right hippocampal connectivity (ALC: $r = -0.39$, $P = 0.042$; CTL: $r = 0.23$, ns; interaction: $z = -3.14$, $P = 0.002$). For the EC network, lower verbal IQ in ALC was associated with weaker SFG–MCC connectivity (ALC: $r = 0.48$, $P = 0.011$; CTL: $r = -0.01$, ns; interaction: $z = 2.6$, $P = 0.009$) and for the SA network, with more restricted ACC–MCC ($r = 0.39$, $P = 0.046$; CTL: $r = 0.07$, ns; $z = 1.67$, $P = 0.09$) and ACC–left IPL connectivity ($r = 0.65$, $P < 0.0001$; CTL: $r = 0.18$, ns; $z = 2.94$, $P = 0.003$). Although only the ACC–left IPL connectivity relationship survived correction for multiple comparisons, these correlations in alcoholics differed significantly from those in controls, except for the ACC–MCC connectivity. To test whether premorbid factors explained connectivity differences between groups, we used education, SES, and verbal IQ as covariates in multivariate analyses of covariance (MANCOVAs) for the DMN, EC, and SA networks and found that group differences (ALC vs. CTL) remained stable for each network (DMN: Pillai's trace $F_{5,43} = 8.49$; $P < 0.0001$; EC network: Pillai's trace $F_{6,42} = 13.6$; $P < 0.0001$; SA network: Pillai's trace $F_{7,41} = 5.20$; $P < 0.0001$), and cluster (all *P*s < 0.05).

To test the relation between "tobacco smoking" and interregional connectivity strength, we used a multivariate analysis of variance (MANOVA) with smoking history as grouping variable: nonsmoking controls ($n = 23$), alcoholic smokers ($n = 15$), and alcoholic nonsmokers ($n = 12$) (Pillai's trace for group: $F_{4,94} = 10.48$, $P < 0.016$) and post hoc least square difference (LSD) analyses for between-group differences. Weaker connectivity strength in ALC than CTL was even weaker in smoking alcoholics driving the group difference in the DMN in regions with restricted PCC–ACC/mPFG connectivity ($F_{2,47} = 3.50$, $P = 0.038$; post hoc LSD test: ALC $P = 0.082$, smoking ALC $P = 0.017$), in the AT network for restricted SPL–left cerebellum ($F_{2,47} = 7.18$, $P = 0.002$; post hoc LSD test: ALC $P = 0.063$, smoking ALC $P < 0.0001$) and SPL–left orbitofrontal connectivity ($F_{2,47} = 4.48$,

Table 6

Pearson correlation results between mood measures and connectivity strength in whole group (ALL), alcoholics (ALC), controls (CTL), and interactions between the 2 groups, for regions of interest (ROI) by group differences in functional connectivity

Analysis	Connectivity	Seed—ROI	Mood		ALL	ALC	CTL	Interaction
Executive control network								
Group contrast	ALC > CTL	SFG—Cuneus	BDI-2	*r*	**0.57***	**0.40**	0.18	$z = 0.82$
				P	**0.0001**	**0.05**	ns	0.21
	CTL > ALC	SFG—MCC	STAI-T	*r*	**−0.42***	**−0.44**	0.24	***z* = −2.43**
				P	**0.002**	**0.025**	ns	**0.008**
Masked contrast	Restricted	SFG—MCC	BDI-2	*r*	**−0.64***	**−0.53***	−0.37	$z = 0.68$
				P	**0.0001**	**0.007**	0.078	0.25
			STAI-S	*r*	**−0.40***	**−0.40**	−0.12	$z = -1.03$
				P	**0.004**	**0.045**	Ns	0.15
Attention network								
Masked contrast	Expanded	SPL—IMFG	BDI-2	*r*	0.08	**−0.43**	0.13	***z* = −2.02**
				P	ns	**0.03**	ns	**0.022**
Reward network								
Group contrast	CTL > ALC	NAcc—lAmygdala	Rosenberg	*r*	**0.52***	**0.41**	0.20	$z = 0.82$
				P	**0.0001**	**0.033**	ns	0.21
		NAcc—lIPL	BDI-2	*R*	**−0.62***	**−0.55***	0.01	***z* = −2.16**
				P	**0.0001**	**0.004**	ns	**0.015**
Masked contrast	Expanded	NAcc—mPFC	STAI-T	*r*	**0.48***	**0.43**	0.09	$z = 1.27$
				P	**0.0001**	**0.027**	ns	0.1
	Restricted	NAcc—lAmygdala	ACQ-R	*r*	**−0.54***	**−0.61***	0.04	***z* = −2.57**
				P	**0.0001**	**0.001**	ns	**0.005**
Somatosensory network								
Masked contrast	Restricted	Postcentral—lTPJ	Rosenberg	*r*	**0.33**	**0.50***	−0.30	***z* = 2.95**
				P	**0.016**	**0.009**	Ns	**0.0016**
Visual network								
Masked contrast	Expanded	Calcarine—lMOG/MTG	Rosenberg	*r*	**−0.48***	**−0.43**	−0.17	$z = -0.99$
				P	**0.0001**	**0.025**	ns	0.16
		Calcarine—Inf OFG	Rosenberg	*r*	**−0.48***	**−0.50***	0.05	***z* = −2.05**
				P	**0.0001**	**0.008**	ns	**0.02**

Notes: Becks Depression Inventory-II total score (BDI) (Beck et al. 1996); Alcohol Craving Quesionnaire (ACQ-R) Short Form (Drobes and Thomas 1999); State-Trait Anxiety Inventory (STAI), trait anxiety (-T), state anxiety (-S) (Spielberger 1983); Self-esteem Scale (Rosenberg 1989). The Barratt Impulsivity Scale (BIS) (Barratt et al. 1995) measure did not correlate with the connectivity strength of regions that were differently connected in alcoholics relative to controls.

For ROIs derived from group contrast analysis (see Table 4), the direction of connectivity differences is indicated by ALC > CTL and CTL > ALC; for ROIs derived from masked contrast analysis (see Table 3), the direction of connectivity differences is indicated by 'expanded' and 'restricted' in ALC relative to controls.

MCC, middle cingulate cortex; SFG, superior frontal gyrus; MFG, middle frontal gyrus; mFG, medial frontal gyrus; Inf OFG, inferior orbitofrontal gyrus; SPL, superior parietal lobe; IPL, inferior parietal lobe; TPJ, temporoparietal junction; IOG, inferior occipital gyrus; MOG, middle occipital gyrus; MTG, middle temporal gyrus.

*Significant FDR corrected for multiple comparisons (Benjamini et al. 2001).

$P = 0.017$; post hoc LSD test: ALC $P = 0.07$, smoking ALC $P = 0.006$), and in the VI network for more restricted calcarine–precentral connectivity ($F_{2,47} = 4.25$, $P = 0.02$; post hoc LSD test: ALC $P = 0.058$, smoking ALC $P = 0.009$). In contrast, more expanded connectivity patterns in ALC, not evident in CTL, were attenuated by smoking in the DMN for the PCC–right MTG connectivity ($F_{2,47} = 7.08$, $P = 0.002$; post hoc LSD test: ALC $P = 0.001$, smoking ALC $P = 0.07$), and in the SS network for postcentral–occipital ($F_{2,47} = 3.04$, $P = 0.05$; post hoc LSD test: ALC $P = 0.018$, smoking ALC, ns) and postcentral–SPL connectivity ($F_{2,47} = 4.87$, $P = 0.012$; post hoc LSD test: ALC $P = 0.004$, smoking ALC $P = 0.075$). We used ANCOVAs to test whether tobacco smoking accounted significantly for the observed functional connectivity differences between groups; group differences remained stable for each network: DMN: Pillai's trace $F_{5,46} = 7.32$; $P < 0.0001$; AT network: Pillai's trace $F_{8,43} = 5.30$; $P < 0.0001$; VI network: Pillai's trace $F_{7,44} = 7.52$; $P < 0.0001$; SS network: Pillai's trace $F_{8,43} = 3.80$; $P = 0.002$), and most cluster (Ps < 0.05), except for 1 cluster of the DMN: PCC–medial prefrontal ($F_{1,50} = 2.69$, $P = 0.11$), and 2 clusters in the AT network: SPL–left cerebellum ($F_{1,50} = 1.38$, $P = 0.25$), and SPL–right temporal pole ($F_{1,50} = 2.21$, $P = 0.14$). Thus, tobacco smoking did not explain main functional network differences between alcoholics and controls but significantly accounted for the variance between groups for PCC–medial prefrontal connectivity in the DMN, and SPL–cerebellar and temporal lobe connectivity in the AT network.

Finally, we tested the relation between "nonalcohol drug use" and interregional connectivity strength using a MANOVA with controls ($n = 26$), alcoholics without drug use co-morbidity (ALC, $n = 14$), and ALC with drug use (ALC + D, $n = 13$) as the grouping variable (Pillai's trace for group: $F_{8,96} = 3.71$, $P = 0.026$) and conducted post hoc LSD analyses for between-group differences. Connectivity was similar in alcoholics with and without drug use for all regions (all Ps > 0.05). Connectivity differences between ALC and CTL remained significant for both ALC subgroups (ALC vs. CTL, ALC + D vs. CTL; post hoc LSD, all Ps < 0.05) except for 2 regions in the AT network for which ALC but not ALC + D differed from controls: SPL–left cerebellum ($F_{2,47} = 6.24$, $P = 0.004$; post hoc LSD test: ALC $P = .001$, ALC + D ns) and SPL–left orbitofrontal connectivity ($F_{2,47} = 5.28$, $P = 0.008$; post hoc LSD test: ALC $P = 0.002$, ALC + D $P = 0.11$). When using an ANCOVA with nonalcohol drug use as covariate, we found the group difference confirmed for all clusters (Ps < 0.05) of the AT network (Pillai's trace $F_{7,44} = 7.52$; $P < 0.0001$).

Discussion

Functional relationships within the living human brain demonstrate consistent patterns of well-organized ongoing, intrinsic activity across both space and time (Biswal et al. 1995; Greicius et al. 2003; Fox et al. 2005; Fox and Raichle 2007; Raichle 2011). The basic level of organization within 9 intrinsic resting-state functional brain networks was preserved in individuals

with chronic alcoholism. Despite this substantial overlap in the intrinsic functional network organization, alcoholics showed network-specific patterns of functional connectivity differing in strength and spatial extent from controls that had behavioral and emotional correlates.

While weaker and restricted interregional activation synchrony in any network generally related to poorer performance and mood states in alcoholics, the relationship between greater and expanded connectivity performance and mood was network-specific. For the default mode, EC, and SA networks, greater and more expanded connectivity was related to poorer performance. Alcoholics appeared to have difficulty confining neural coherence within these networks and were synchronously activating regions outside these specialized systems. This may be seen as a form of functional network dedifferentiation in alcoholism (Kramer et al. 1989; Schulte et al. 2010b), similar to dedifferentiation processes in aging that are marked by less distinctive activation patterns in frontal and posterior brain regions and less effective transfer of information from one region to the next (Goh 2011). In contrast, greater and more extended connectivity in AT and VI networks in alcoholics were indicative of neural compensatory mechanisms to overcome impairment and achieve better performance levels.

Self-referential Functional Networking in Alcoholism

For the DMN, the main connected nodes of the PCC were bilateral medial and dorsolateral prefrontal and temporoparietal cortices, with the addition of cerebellar regions, consistent with the main DMN regions described in healthy subjects (Biswal et al. 1995; Buckner et al. 2008; Fox et al. 2005) and alcoholics (Chanraud et al. 2011). Although we found substantial overlap in DMN connectivity maps of alcoholics and controls, group differences emerged for greater PCC–occipital cortex and weaker PCC–caudate connectivity. Alcoholics further showed restricted connectivity to bilateral medial prefrontal regions, consistent with previous reports (Courtney et al. 2013), and more expanded connectivity to superior, middle, and medial temporal gyri. This is particularly notable for the hippocampus given the relatively small size of the structure. Parts of the hippocampal formation (Raichle and Snyder 2007; Buckner et al. 2008) and the temporal lobe (Sämann et al. 2011) have been inconsistently reported as regions of the DMN suggesting a loose integration into this network in healthy controls. During the resting state, hippocampal regions seem to lack a direct functional connection with cortical DMN nodes, but are indirectly connected with the PCC via the parahippocampal gyrus (Ward et al. 2014). Our finding that hippocampal network expansion and weaker PCC–caudate connectivity strength in alcoholics correlated with lower verbal IQ suggests that premorbid factors shape DM networking, even though they did not contribute significantly to the observed between-group variance in DMN connectivity. Considering the reciprocal relationships of DMN connectivity during task and resting state (Andrews-Hanna et al. 2010), and the role of alternative DMN pathways for performance enhancement during task processing (Chanraud et al. 2011, 2012), the observed DMN pattern in alcoholics may signify inefficient neural networking, potentially occurring premorbidly, for integrating and utilizing neurofunctional resources.

Integrative Functional Networking in Alcoholism

The EC network is a prominent network that subserves a wide range of cognitive control functions and is associated with the dlPFC as the main network node located in middle and SFG. The EC network is affected in alcohol-dependent individuals contributing to dysfunctions in conflict processing, error monitoring, and response inhibition (Fein and Di Sclafani 2004).

Nevertheless, during rest, alcoholics and controls showed a substantial overlap in SFG connectivity to bilateral lateral and medial parietal, temporal, and cerebellar regions. Compared with controls, alcoholics showed expanded connectivity to medial frontal, right temporal, and cuneus/extrastriate cortical regions, and restricted connectivity with left parietal and inferior frontal regions in addition to weaker connectivity with MCC, insula, and caudate body areas. Weaker and restricted SFG–MCC connectivity correlated with higher depression and anxiety scores, and slower perceptual-motor processing speed, particularly in alcoholics relative to controls, and was associated with younger age at alcoholism onset. A recent fMRI study (Schulte et al. 2012) showed that the MCC plays a role in modulating the frontoparietal EC system to adapt to the need of flexibly switching responses during Stroop conflict processing. Here, alcoholics exhibited weaker PCC–MCC connectivity and greater midbrain–MCC connectivity than controls, especially for response switches, than controls. Thus, MCC connectivity appears to be a neural mechanism participating in the modulation of regional networking to changing EC demands. That SFG–MCC connectivity during rest was even weaker in alcoholics with earlier alcoholism onset further suggests vulnerability of these network dynamics involved in an optimal balance between cognitive labor and leisure (see, e.g., Kool and Botvinick 2014), that is, between mind wandering and EC. A pronounced reduction of this network capability, whether as a predisposition or consequence of alcoholism, can potentially impede cognition and emotional well-being.

Closely associated with the EC network is the SA network. Activity in the ACC has been associated with SA, as in the detection of errors and novel stimuli (Carter et al. 1998), motivational SA (Harsay et al. 2012), EM and RW (Nishijo et al. 1997; Bush et al. 2000, 2002), and when performance monitoring becomes necessary (Ridderinkhof et al. 2004). Consistent with other studies, synchronous activity in the ACC-based SA network involved medial and inferior frontal, insular (Taylor et al. 2009), and parietal regions (Downar et al. 2002), and the striatum (caudate, putamen) (Gradin et al. 2013), and was highly overlapping in alcoholics and controls. Alcoholics showed greater and more expanded frontostriatal SA network connectivity involving the caudate nucleus and medial, inferior frontal regions, more expanded connectivity with orbitofrontal regions, and further exhibited thalamo-cortical network reduction including weaker and restricted connectivity with the thalamus, medial superior frontal, MCC, and cuneus regions, with most of them related to poorer verbal and visuospatial working memory. Weaker ACC–MCC and restricted ACC–left IPL connectivity was further related to lower verbal IQ in alcoholics, but not in controls, suggesting that SA network reduction in alcoholics was modulated by premorbid factors, even though they did not explain the group difference in interregional connectivity. Disruption of functional network connectivity between frontostriatal network nodes relevant for response inhibition has been previously demonstrated in chronic alcoholics (Courtney et al. 2013; Müller-Oehring et al. 2013). Our study demonstrates that, even during rest, ACC-seeded connectivity, and especially reduced synchrony, is highly predictive of performance level in abstinent alcoholics.

Chronic alcohol consumption can affect AT by limiting the capacity to process goal-relevant information and impeding frontoparietal circuitry (Petit et al. 2012). In the current study, connectivity analyses confirmed SPL–occipital and SPL–frontal connectivity in both groups, with weaker connectivity to temporal regions and extended connectivity to superior occipital, parietal, and frontal regions. A moderate correlation indicated fewer depressive symptoms with more expanded SPL–left MFG connectivity in alcoholics and provided limited support for a compensatory role of AT network expansion.

"Primary input function network" showed some differences in strength and expansion of connectivity patterns in alcoholics compared with controls that were more pronounced in the SS network and least evident in the AU network. Only in the VI network was more expanded calcarine–inferior orbitofrontal connectivity related to better visuospatial working memory performance implicating compensatory recruitment to support a specific function maintained by this network. Overall, primary input functional networks appeared to be less vulnerable to the effects of alcohol than integrative functional networks.

Subcortical Emotion and Reward Functional Networking in Alcohol Dependence

Networks comprising EM with the amygdala as the main node (Hariri et al. 2003), and RW with the ventral striatum, in particular the NAcc (Cauda et al. 2011), as a main node, have been implicated in chronic alcoholism (Makris et al. 2008; Schulte et al. 2010a; O'Daly et al. 2012). Herein, EM network connectivity was highly similar in alcoholics and controls with only minor variations. Nonetheless, the RW network showed significantly extended frontostriatal (medial prefrontal/caudate) connectivity and less synchronized activity to limbic (amygdala, hippocampus) and parietal regions in alcoholics, which was associated with higher anxiety, more depressive symptoms, and increased alcohol craving, particularly in alcoholics relative to controls. Together, these associations suggest a role for RW system functional integrity in EM regulation and potentially relapse prediction (Camchong et al. 2013b).

These functional brain network data provide initial evidence for alcohol-related effects on multiple intrinsic networks; yet, alcoholism today often occurs in concert with other addictions. Although we did not find indication that the observed connectivity differences in alcoholics were driven by additional nonalcohol drug use, tobacco smoking was a relevant factor associated with weaker and more restricted interregional connectivity within DMN, AT, and VI networks. In addition, for the DMN, SA, and EC networks, we found evidence for premorbid estimates of cognitive ability in alcoholics to shape interregional connectivity, potentially contributing to neurofunctional vulnerability of networks relevant for addictive behaviors.

Conclusion

Overall, our findings provide evidence that alcoholism affects the resting default mode, EC, SA, AT, RW, and SS networks, but leaves EM, VI, and AU networks relatively spared when not performing a directed task. The observed alcohol-related connectivity differences reflect altered functional organization in multiple networks, which can impair preparation for switching between network functions and for exerting EC when needed. For only the AT and VI networks did our data compare with previous evidence for better task performance heralded by greater connectivity in alcoholism. Disruption of these 2 networks may be a mechanism underlying the commonly detected alcoholism-related impairments of selective AT and visuospatial processing supported by these networks. Pattern of extended connectivity in alcoholism to regions outside the main networks suggests that the neural representations underlying different cognitive and emotional processes become less selective and their neural signature less distinct. We propose that this constellation of altered intrinsic networking is a biological marker of chronic alcoholism and mechanism to explain signature impairments in EC, cognitive switching, RW evaluation, and visuospatial processing.

Funding

NIH Grants R01 AA018022, AA012388, and AA017168 funded this work.

Notes

We thank Stephanie Sassoon, Priya Asok, Karen Jackson, and Crystal Caldwell for help with recruitment and clinical interviewing, William Hawkes for help with scheduling and data acquisition, and Margaret Rosenbloom for comments on the manuscript. *Conflict of Interest*: None declared.

References

Andrews-Hanna JR, Reidler JS, Sepulcre J, Poulin R, Buckner RL. 2010. Functional-anatomic fractionation of the brain's default network. Neuron. 65:550–562.

Anticevic A, Cole M, Murray J, Corlett P, Wang X, Krystal J. 2012. The role of default network deactivation in cognition and disease. Trends Cogn Sci. 16:584–592.

Anticevic A, Cole MW, Repovs G, Murray JD, Brumbaugh MS, Winkler AM, Savic A, Krystal JH, Pearlson GD, Glahn DC. 2015. Characterizing thalamo-cortical disturbances in schizophrenia and bipolar illness. Cereb Cortex. 24:3116–3130.

Babor T, Higgins-Biddle J, Saunders J, Monteiro M. 2006. AUDIT: The Alcohol Use Disorders Identification Test: guidelines for use in primary care. Geneva, Switzerland: World Health Organization.

Bach M. 2007. The Freiburg Visual Acuity Test-variability unchanged by post-hoc re-analysis. Graefes Arch Clin Exp Ophthalmol. 245:965–971.

Barratt ES, Patton J, Stanford M. 1995. Barratt Impulsiveness Scale. New York: Plenum Press.

Bechara A. 2005. Decision making, impulse control and loss of willpower to resist drugs: a neurocognitive perspective. Nat Neurosci. 8:1458–1463.

Beck A, Steer R, Brown G. 1996. Manual for the Beck Depression Inventory-II. San Antonio (TX): Psychological Corporation.

Beck A, Wüstenberg T, Genauck A, Wrase J, Schlagenhauf F, Smolka M, Mann K, Heinz A. 2012. Effect of brain structure, brain function, and brain connectivity on relapse in alcohol-dependent patients. Arch Gen Psychiatry. 69:842–852.

Benjamini Y, Drai D, Elmer G, Kafkafi N, Golani I. 2001. Controlling the false discovery rate in behavior genetics research. Behav Brain Res. 125:279–284.

Berridge K, Robinson T. 1998. What is the role of dopamine in reward: hedonic impact, reward learning, or incentive salience? Brain Res Brain Res Rev. 28:309–369.

Biswal B, Yetkin F, Haughton V, Hyde J. 1995. Functional connectivity in the motor cortex of resting human brain using echo-planar MRI. Magn Reson Med. 34:537–541.

Biswal BB, Mennes M, Zuo X-N, Gohel S, Kelly C, Smith SM, Beckmann CF, Adelstein JS, Buckner RL, Colcombe S. 2010. Toward discovery science of human brain function. Proc Natl Acad Sci USA. 107:4734–4739.
Buckner R, Andrews-Hanna J, Schacter D. 2008. The brain's default network: anatomy, function, and relevance to disease. Ann N Y Acad Sci. 1124:1–38.
Bush G, Luu P, Posner M. 2000. Cognitive and emotional influences in anterior cingulate cortex. Trends Cogn Sci. 4:215–222.
Bush G, Vogt B, Holmes J, Dale A, Greve D, Jenike M, Rosen B. 2002. Dorsal anterior cingulate cortex: a role in reward-based decision making. Proc Natl Acad Sci USA. 99:523–528.
Cabeza R. 2002. Hemispheric asymmetry reduction in older adults: the HAROLD model. Psychol Aging. 17:85–100.
Cabeza R, Anderson N, Locantore J, McIntosh A. 2002. Aging gracefully: compensatory brain activity in high-performing older adults. NeuroImage. 17:1394–1402.
Cabeza R, Nyberg L, Park D. 2005. Cognitive neuroscience of aging: linking cognitive and cerebral aging. New York (NY): Oxford University Press.
Camchong J, Stenger A, Fein G. 2013a. Resting-state synchrony during early alcohol abstinence can predict subsequent relapse. Cereb Cortex. 23:2086–2099.
Camchong J, Stenger A, Fein G. 2013b. Resting-state synchrony in long-term abstinent alcoholics. Alcohol Clin Exp Res. 7:75–85.
Camchong J, Stenger V, Fein G. 2013c. Resting-state synchrony in short-term versus long-term abstinent alcoholics. Alcohol Clin Exp Res. 37:794–803.
Carter C, Braver T, Barch D, Botvinick M, Noll D, Cohen J. 1998. Anterior cingulate cortex, error detection, and the online monitoring of performance. Science. 280:747–749.
Cauda F, Cavanna A, D'agata F, Sacco K, Duca S, Geminiani G. 2011. Functional connectivity and coactivation of the nucleus accumbens: a combined functional connectivity and structure-based meta-analysis. J Cogn Neurosci. 23:2864–2877.
Chanraud S, Pitel A, Müller-Oehring E, Pfefferbaum A, Sullivan E. 2012. Remapping the brain to compensate for impairment in recovering alcoholics. Cereb Cortex. 23:97–104.
Chanraud S, Pitel A-L, Pfefferbaum A, Sullivan EV. 2011. Disruption of functional connectivity of the default-mode network in alcoholism. Cereb Cortex. 21:2272–2281.
Courtney K, Ghahremani D, Ray L. 2013. Fronto-striatal functional connectivity during response inhibition in alcohol dependence. Addict Biol. 18:593–604.
Crovitz HF, Zener KA. 1962. Group test for assessing hand and eye dominance. Am J Psychol. 75:271–276.
Demos K, Heatherton T, Kelley W. 2012. Individual differences in nucleus accumbens activity to food and sexual images predict weight gain and sexual behavior. J Neurosci. 32:5549–5552.
Downar J, Crawley A, Mikulis D, Davis K. 2002. A cortical network sensitive to stimulus salience in a neutral behavioral context across multiple sensory modalities. J Neurophysiol. 87:615–620.
Drobes D, Thomas S. 1999. Assessing craving for alcohol. Alcohol Res Health. 23:179–186.
Fein G, Di Sclafani V. 2004. Cerebral reserve capacity: implications for alcohol and drug abuse. Alcohol. 32:63–67.
First MB, Spitzer RL, Gibbon M, Williams JB. 2012. Structured Clinical Interview for DSM-IV Axis I Disorders (SCID-I), Clinician Version, Administration Booklet. Washington, D.C.: American Psychiatric Press, Inc.
Folstein MF, Folstein S. 2010. Mini-Mental State Examination, 2nd Edition (MMSE-2). Lutz (FL): PAR.
Fox M, Raichle M. 2007. Spontaneous fluctuations in brain activity observed with functional magnetic resonance imaging. Nat Rev Neurosci. 8:700–711.
Fox M, Snyder A, Vincent J, Corbetta M, Van Essen D, Raichle M. 2005. The human brain is intrinsically organized into dynamic, anticorrelated functional networks. Proc Natl Acad Sci USA. 102:9673–9678.
Goh JO. 2011. Functional dedifferentiation and altered connectivity in older adults: neural accounts of cognitive aging. Aging Dis. 2:30–48.
Gradin V, Waiter G, O'Connor A, Romaniuk L, Stickle C, Matthews K, Hall J, Douglas SJ. 2013. Salience network-midbrain dysconnectivity and blunted reward signals in schizophrenia. Psychiatry Res. 211:104–111.
Greicius MD, Krasnow B, Reiss AL, Menon V. 2003. Functional connectivity in the resting brain: a network analysis of the default mode hypothesis. Proc Natl Acad Sci USA. 100:253–258.
Hariri A, Mattay V, Tessitore A, Fera F, Weinberger D. 2003. Neocortical modulation of the amygdala response to fearful stimuli. Biol Psychiatry. 53:494–501.
Harsay H, Spaan M, Wijnen J, Ridderinkhof K. 2012. Error awareness and salience processing in the oddball task: shared neural mechanisms. Front Hum Neurosci. 6:246.
Hollingshead A, Redlich F. 1958. Social class and mental illness. New York: Wiley.
Kamarajan C, Porjesz B, Jones K, Choi K, Chorlian D, Padmanabhapillai A, Rangaswamy M, Stimus A, Begleiter H. 2004. The role of brain oscillations as functional correlates of cognitive systems: a study of frontal inhibitory control in alcoholism. Int J Psychophysiol. 51:155–180.
Kool W, Botvinick M. 2014. A labor/leisure tradeoff in cognitive control. J Exp Psychol Gen. 143:131–141.
Kramer J, Blusewicz M, Preston K. 1989. The premature aging hypothesis: old before its time? J Consult Clin Psychol. 57:257–262.
Laird A, Fox P, Eickhoff S, Turner J, Ray K, McKay D, Glahn D, Beckmann C, Smith S, Fox P. 2011. Behavioral interpretations of intrinsic connectivity networks. J Cogn Neurosci. 23:4022–4037.
Leech R, Kamourieh S, Beckmann C, Sharp D. 2011. Fractionating the default mode network: distinct contributions of the ventral and dorsal posterior cingulate cortex to cognitive control. J Neurosci. 31:3217–3224.
Loeber S, Duka T, Welzel H, Nakovics H, Heinz A, Flor H, Mann K. 2009a. Impairment of cognitive abilities and decision making after chronic use of alcohol: the impact of multiple detoxifications. Alcohol Alcohol. 44:372–381.
Loeber S, Vollstadt-Klein S, von der Goltz C, Flor H, Mann K, Kiefer F. 2009b. Attentional bias in alcohol-dependent patients: the role of chronicity and executive functioning. Addict Biol. 14:194–203.
Makris N, Oscar-Berman M, Kim S, Hodge SM, Kennedy DN, Caviness VS, Marinkovic K, Breiter HC, Gasic GP, Harris GJ. 2008. Decreased volume of the brain reward system in alcoholism. Biol Psychiatry. 64:192–202.
Marinkovic K, Oscar-Berman M, Urban T, O'Reilly C, Howard J, Sawyer K, Harris G. 2009. Alcoholism and dampened temporal limbic activation to emotional faces. Alcohol Clin Exp Res. 33:1880–1892.
Müller-Oehring EM, Jung Y-C, Sullivan EV, Hawkes WC, Pfefferbaum A, Schulte T. 2013. Midbrain-driven emotion and reward processing in alcoholism. Neuropsychopharmacology. 38:1844–1853.
Neto L, Oliveira E, Correia F, Ferreira A. 2008. The human nucleus accumbens: where is it? A stereotactic, anatomical and magnetic resonance imaging study. Neuromodulation. 11:13–22.
Nishijo H, Yamamoto Y, Ono T, Uwano T, Yamashita J, Yamashima T. 1997. Single neuron responses in the monkey anterior cingulate cortex during visual discrimination. Neurosci Lett. 227:79–82.
O'Daly OG, Trick L, Scaife J, Marshall J, Ball D, Phillips ML, Williams SS, Stephens DN, Duka T. 2012. Withdrawal-associated increases and decreases in functional neural connectivity associated with altered emotional regulation in alcoholism. Neuropsychopharmacology. 37:2267–2276.
Park SQ, Kahnt T, Beck A, Cohen MX, Dolan RJ, Wrase J, Heinz A. 2010. Prefrontal cortex fails to learn from reward prediction errors in alcohol dependence. J Neurosci. 30:7749–7753.
Parks M, Greenberg D, Nickel M, Dietrich M, Rogers B, Martin P. 2010. Recruitment of additional brain regions to accomplish simple motor tasks in chronic alcohol-dependent patients. Alcohol Clin Exp Res. 34:1098–1109.
Petit Gr, Kornreich C, Noël X, Verbanck P, Campanella S. 2012. Alcohol-related context modulates performance of social drinkers in a visual Go/No-Go Task: a preliminary assessment of event-related potentials. PLoS One. 7:e37466.

Pfefferbaum A, Chanraud S, Pitel A-L, Müller-Oehring E, Shankaranarayanan A, Alsop DC, Rohlfing T, Sullivan EV. 2011. Cerebral blood flow in posterior cortical nodes of the default mode network decreases with task engagement but remains higher than in most brain regions. Cereb Cortex. 21:233–244.

Phan K, Wager T, Taylor S, Liberzon I. 2002. Functional neuroanatomy of emotion: a meta-analysis of emotion activation studies in PET and fMRI. Neuroimage. 16:331–348.

Poline J, Worsley K, Evans A, Friston K. 1997. Combining spatial extent and peak intensity to test for activations in functional imaging. Neuroimage. 5:83–96.

Raabe A, Grüsser S, Wessa M, Podschus J, Flor H. 2005. The assessment of craving: psychometric properties, factor structure and a revised version of the Alcohol Craving Questionnaire (ACQ). Addiction. 100:227–234.

Raichle M, Snyder A. 2007. A default mode of brain function: a brief history of an evolving idea. Neuroimage. 37:1083–1090.

Raichle ME. 2011. The restless brain. Brain Connect. 1:3–12.

Reitan RM, Wolfson D. 1985. The Halstead-Reitan neuropsychological test battery: Theory and clinical interpretation. Tucson (AZ): Neuropsychology Press.

Reuter-Lorenz P, Jonides J, Smith E, Hartley A, Miller A, Marshuetz C, Koeppe R. 2000. Age differences in the frontal lateralization of verbal and spatial working memory revealed by PET. J Cogn Neurosci. 12:174–187.

Ridderinkhof K, van den Wildenberg W, Segalowitz S, Carter C. 2004. Neurocognitive mechanisms of cognitive control: the role of prefrontal cortex in action selection, response inhibition, performance monitoring, and reward-based learning. Brain Cogn. 56:129–140.

Rogers B, Parks M, Nickel M, Katwal S, Martin P. 2012. Reduced fronto-cerebellar functional connectivity in chronic alcoholic patients. Alcohol Clin Exp Res. 36:294–301.

Rosenberg M. 1989. Society and the adolescent self-image. Middletown (CT): Wesleyan University Press.

Sämann PG, Wehrle R, Hoehn D, Spoormaker VI, Peters H, Tully C, Holsboer F, Czisch M. 2011. Development of the brain's default mode network from wakefulness to slow wave sleep. Cereb Cortex. 21:2082–2093.

Schulte T, Müller-Oehring EM, Pfefferbaum A, Sullivan EV. 2010a. Neurocircuitry of emotion and cognition in alcoholism: contributions from white matter fiber tractography. Dialogues Clin Neurosci. 12:554–560.

Schulte T, Müller-Oehring EM, Rohlfing T, Pfefferbaum A, Sullivan EV. 2010b. White matter fiber degradation attenuates hemispheric asymmetry when integrating visuomotor information. J Neurosci. 30:12168–12178.

Schulte T, Müller-Oehring EM, Sullivan EV, Pfefferbaum A. 2012. Synchrony of corticostriatal-midbrain activation enables normal inhibitory control and conflict processing in recovering alcoholic men. Biol Psychiatry. 71:269–278.

Smith SM, Fox PT, Miller KL, Glahn DC, Fox PM, Mackay CE, Filippini N, Watkins KE, Toro R, Laird AR. 2009. Correspondence of the brain's functional architecture during activation and rest. Proc Natl Acad Sci USA. 106:13040–13045.

Spielberger C. 1983. State-Trait Anxiety Inventory STAI (Form Y). Palo Alto (CA): Consulting Psychologists Press, Inc.

Sullivan EV, Müller-Oehring EM, Pitel A-L, Chanraud S, Shankaranarayanan A, Alsop DC, Rohlfing T, Pfefferbaum A. 2013. A selective insular perfusion deficit contributes to compromised salience network connectivity in recovering alcoholic men. Biol Psychiatry. 74:547–555.

Taylor K, Seminowicz D, Davis K. 2009. Two systems of resting state connectivity between the insula and cingulate cortex. Hum Brain Mapp. 30:2731–2745.

Tzourio-Mazoyer N, Landeau B, Papathanassiou D, Crivello F, Etard O, Delcroix N, Mazoyer B, Joliot M. 2002. Automated anatomical labeling of activations in SPM using a macroscopic anatomical parcellation of the MNI MRI single-subject brain. Neuroimage. 15:273–289.

Ward A, Schultz A, Huijbers W, Van Dijk K, Hedden T, Sperling R. 2014. The parahippocampal gyrus links the default-mode cortical network with the medial temporal lobe memory system. Hum Brain Mapp. 35:1061–1073.

Wechsler D. 2001. Wechsler Test of Adult Reading: WTAR. San Antonio (TX): Pearson Education, Inc.

Wechsler D. 1987. WMS-R: Wechsler Memory Scale-Revised: Manual. San Antonio (TX): Psychological Corporation San Antonio.

Whitfield-Gabrieli S, Nieto-Castanon A. 2012. Conn: a functional connectivity toolbox for correlated and anticorrelated brain networks. Brain Connect. 2:125–141.

WHO. 2011. Global status report on alcohol and health. Le Mont-sur-Lausanne, Switzerland: WHO Library Cataloguing-in-Publication Data.

Yoder KK, Morris ED, Constantinescu CC, Cheng T-E, Normandin MD, O'Connor SJ, Kareken DA. 2009. When what you see isn't what you get: alcohol cues, alcohol administration, prediction error, and human striatal dopamine. Alcohol Clin Exp Res. 33:139–149.